

KRONOS & KRIOS: EVIDENCE FOR ACCRETION OF A MASSIVE, ROCKY PLANETARY SYSTEM IN A COMOVING PAIR OF SOLAR-TYPE STARS

SEMYEONG OH,^{1,2} ADRIAN M. PRICE-WHELAN,¹ JOHN M. BREWER,^{3,4}
DAVID W. HOGG,^{5,6,7,8} DAVID N. SPERGEL,^{1,5} AND JUSTIN MYLES³

¹*Department of Astrophysical Sciences, Princeton University, 4 Ivy Lane, Princeton, NJ 08544, USA*

²*To whom correspondence should be addressed: semyeong@astro.princeton.edu*

³*Department of Astronomy, Yale University, 260 Whitney Ave, New Haven, CT 06511, USA*

⁴*Department of Astronomy, Columbia University, 550 West 120th Street, New York, NY 10027, USA*

⁵*Center for Computational Astrophysics, Flatiron Institute, 162 Fifth Ave, New York, NY 10010, USA*

⁶*Center for Cosmology and Particle Physics, Department of Physics, New York University, 726 Broadway, New York, NY 10003, USA*

⁷*Center for Data Science, New York University, 60 Fifth Ave, New York, NY 10011, USA*

⁸*Max-Planck-Institut für Astronomie, Königstuhl 17, D-69117 Heidelberg*

ABSTRACT

We report and discuss the discovery of a comoving pair of bright solar-type stars, HD 240430 and HD 240429, with a significant difference in their chemical abundances. The two stars have an estimated 3D separation of ≈ 0.6 pc (≈ 0.01 pc projected) at a distance of $r \approx 100$ pc with nearly identical three-dimensional velocities, as inferred from *Gaia* TGAS parallaxes and proper motions, and high-precision radial velocity measurements. Stellar parameters determined from high-resolution Keck HIRES spectra indicate that both stars are ~ 4 Gyr old. The more metal-rich of the two, HD 240430, shows an enhancement of refractory ($T_C > 1200$ K) elements by ≈ 0.2 dex and a marginal enhancement of (moderately) volatile elements ($T_C < 1200$ K; C, N, O, Na, and Mn). This is the largest metallicity difference found in a wide binary pair yet. Additionally, HD 240430 shows an anomalously high surface lithium abundance ($A(\text{Li}) = 2.75$), higher than its companion by 0.5 dex. The proximity in phase-space and ages between the two stars suggests that they formed together with the same composition, at odds with the observed differences in metallicity and abundance patterns. We therefore suggest that the star HD 240430, “Kronos”, accreted $15 M_{\oplus}$ of rocky material after birth, selectively enhancing the refractory elements as well as lithium in its surface and convective envelope.

Keywords: binaries: visual — planet-star interactions — stars: abundances — stars: formation — stars: individual (HD 240430, HD 240429) — stars: solar-type

1. INTRODUCTION

Wide binary stars are valuable tools for studying star and planet formation as well as Galactic dynamics and chemical evolution. In the context of studying the evolution of the Milky Way, they are useful for two main reasons. First, because wide binaries are weakly bound systems that may be tidally disrupted by, e.g., field stars, molecular clouds, or the Galactic tidal field, their statistics can be informative of the Galactic mass distribution. For example, the separation distribution of halo binaries has been used to constrain the mass of massive compact halo objects (Yoo et al. 2004; Quinn et al. 2009; Allen & Monroy-Rodríguez 2014). They can also be used to test the “chemical tagging” hypothesis that stars from the same birthplace may be traced back using detailed chemical abundance patterns as birth tags (Freeman & Bland-Hawthorn 2002). While any multiple-star system, including massive open clusters, can be used to test the hypothesis, wide binaries have the advantage of being extremely abundant, rendering their statistics a meaningful indication of whether the hypothesis works.

Binary stars that form from the same birth cloud start with nearly identical composition. A differential analysis of the chemical composition of binary stars can reveal their history through the chemical signatures related to planet formation or accretion regardless of Galactic chemical evolution. Giant planets on short period orbits have been shown, via population studies, to form more readily around inherently metal rich stars (e.g., Fischer & Valenti 2005; Santos et al. 2004). However, the post-formation accretion of rocky planets can still alter the photospheric abundances. If host stars are polluted after their birth by rocky planetary material with a high refractory-to-volatile ratio, the convective envelope of the stars may be enhanced in refractory elements (e.g., Fe) compared to their initial state (e.g., Pinsonneault et al. 2001). Thus, differences in planet formation or accretion in two otherwise identical stars may imprint differences in chemical abundances that depend on the condensation temperature (T_C).

High resolution spectroscopic studies of binary star systems hosting at least one planet (Ramírez et al. 2011; Tucci Maia et al. 2014; Teske et al. 2013; Mack et al. 2014; Liu et al. 2014; Teske et al. 2015; Saffe et al. 2015; Ramírez et al. 2015; Biazzo et al. 2015; Mack et al. 2016; Teske et al. 2016a,b) have yielded varied results: while some systems appear to have undetectable differences (see also Desidera et al. 2004; Gratton et al. 2001), other studies have reported a T_C -dependent difference in abundance with higher- T_C elements showing larger differences. A possible explanation for the difference is that forming more gas giants or rocky planets leads to an overall or T_C -dependent depletion of metals in gas that eventually accretes onto the host star (Ramírez et al. 2015; Biazzo et al. 2015). Alternatively, late time accretion of refractory-rich planetary material can also produce the trend by enhancing the abundance of high- T_C elements in one of the two stars. The observed differences are $\lesssim 0.1$ dex even in the most dramatic case, and often at a level of ≈ 0.05 dex, making them challenging to detect even with a careful analysis of high-resolution, high signal-to-noise ratio spectra, and differential analyses of two stars that are very similar in their stellar parameters. We

refer the readers to Appendix A for a review of a handful of individual pairs studied in their detailed chemical abundances (see also Melendez & Ramirez 2016).

Spectral analysis of polluted white dwarfs (WDs) currently provides the strongest evidence for accretion of planetary material by a host star (Zuckerman et al. 2003, 2010; Koester et al. 2014; see Farihi 2016 for review). Because the gravitational settling times of elements heavier than He in the WD atmosphere is much shorter than the WD cooling time (Paquette et al. 1986), detection of metals likely indicates the presence of a reservoir of dusty material around the WD. Indeed, many of the polluted WDs host a dusty debris disk detected in the infrared (Zuckerman & Becklin 1987; Graham et al. 1990; Reach et al. 2005; Farihi et al. 2009; Kilic et al. 2006). Some of the most dramatically polluted WDs show surface abundances closely matched by rocky planetary material with, e.g., bulk Earth composition, strongly arguing that the disk formed from tidally disrupted minor planets (Zuckerman et al. 2007; Klein et al. 2010). Recently, transit signals from small bodies orbiting around a polluted WD have been detected by *Kepler* adding further support to the picture (Vanderburg et al. 2015).

Here, we report and discuss the discovery of a comoving pair of G stars, HD 240430 and HD 240429, with unusual chemical abundance differences that strongly suggest accretion of rocky planetary material by one of the two stars, HD 240430. Throughout the Article, we nickname the two stars Kronos (HD 240430) and Krios (HD 240429). In Greek mythology, Kronos and Krios were sons of Uranos and Gaia. Kronos notoriously devoured all of his children (except Zeus) to prevent the prophecy that one day he will be overthrown by them. We use the following convention for chemical abundances of stars: $[X/H]$ is the log ratio of the number density of an element X to H relative to the solar value, $[X/H] = \log_{10}((n_X/n_H)/(n_{X,\odot}/n_{H,\odot}))$. The absolute abundance of an element X is $A(X) = 12 + \log_{10}(n_X/n_H)$. In Section 2 we present the astrometric and spectroscopic data about the two stars relevant to the present discussion. In Section 3 we discuss possible interpretations of the abundance difference between the pair. We summarize our discussions in Section 4.

2. DATA

Krios and Kronos were identified as a candidate comoving star pair in our recent search for comoving stars using the proper motions and parallaxes from the Tycho-Gaia Astrometric Solution catalog (TGAS), a component of *Gaia* DR1. We refer the readers to this previous work (Oh et al. 2017) for a full explanation of the methodology behind this search and only include a brief description here. For a given pair, we compute the marginalized likelihood ratio between the hypotheses (1) that a given pair of stars share the same 3D velocity vector, and (2) that they have independent 3D velocity vectors, using only the astrometric measurements from TGAS (parallaxes and proper motions). We then select a sample of high-confidence comoving pairs by making a conservative cut on this likelihood ratio. In the resulting catalog of comoving pairs (Oh et al. 2017), the pair presented in this paper was assigned a group id of 1199, and the marginalized

Table 1. Astrometric and spectroscopic measurements of the pair

Name	Units	Krios	Kronos	Uncertainties
		HD 240429	HD 240430	
Sp Type		G0	G2	
R.A. ^a	hh:mm:ss	23:51:55.21	23:52:09.42	
Dec. ^a	dd:mm:ss	59:42:48.16	59:42:26.08	
2MASS J^a	mag	8.593 ± 0.023	8.415 ± 0.026	
T_{eff}	K	5878	5803	25
$\log g$		4.43	4.33	0.028
$v \sin i$	km s ⁻¹	1.1	2.5	
[Fe/H]		0.01	0.20	0.010
Age ^b	Gyr	$4.00^{+1.51}_{-1.56}$	$4.28^{+1.11}_{-1.03}$	
v_r	km s ⁻¹	-21.2	-21.2	0.2
ϖ^a	mas	9.35 ± 0.24	9.41 ± 0.25	
μ_{α}^{*a}	mas yr ⁻¹	89.25 ± 0.66	89.41 ± 0.69	
μ_{δ}^a	mas yr ⁻¹	-29.68 ± 0.54	-30.12 ± 0.52	
$T_c < 1200$ K				
$A(\text{Li})^c$		2.25	2.75	0.05
[C/H]		0.00	0.09	0.026
[N/H]		-0.06	-0.01	0.042
[O/H]		0.01	0.09	0.036
[Na/H]		-0.06	-0.04	0.014
[Mn/H]		-0.03	0.00	0.020
$T_c > 1200$ K				
[Mg/H]		0.01	0.19	0.012
[Al/H]		0.01	0.21	0.028
[Si/H]		0.00	0.16	0.008
[Ca/H]		0.02	0.23	0.014
[Ti/H]		0.02	0.20	0.012
[V/H]		0.02	0.20	0.034
[Cr/H]		0.01	0.17	0.014
[Fe/H]		0.01	0.20	0.010
[Ni/H]		-0.01	0.21	0.014
[Y/H]		0.04	0.26	0.030

^aFrom TGAS.^bDerived in this work by isochrone fitting using the Yale-Yonsei model isochrones (Spada et al. 2013; see Section 3.1).^cAbsolute abundances from Myles 2017 in prep.NOTE— All values are from Brewer et al. 2016 unless otherwise noted. The microturbulence parameter is fixed at 0.85 km s⁻¹ (Brewer et al. 2015).

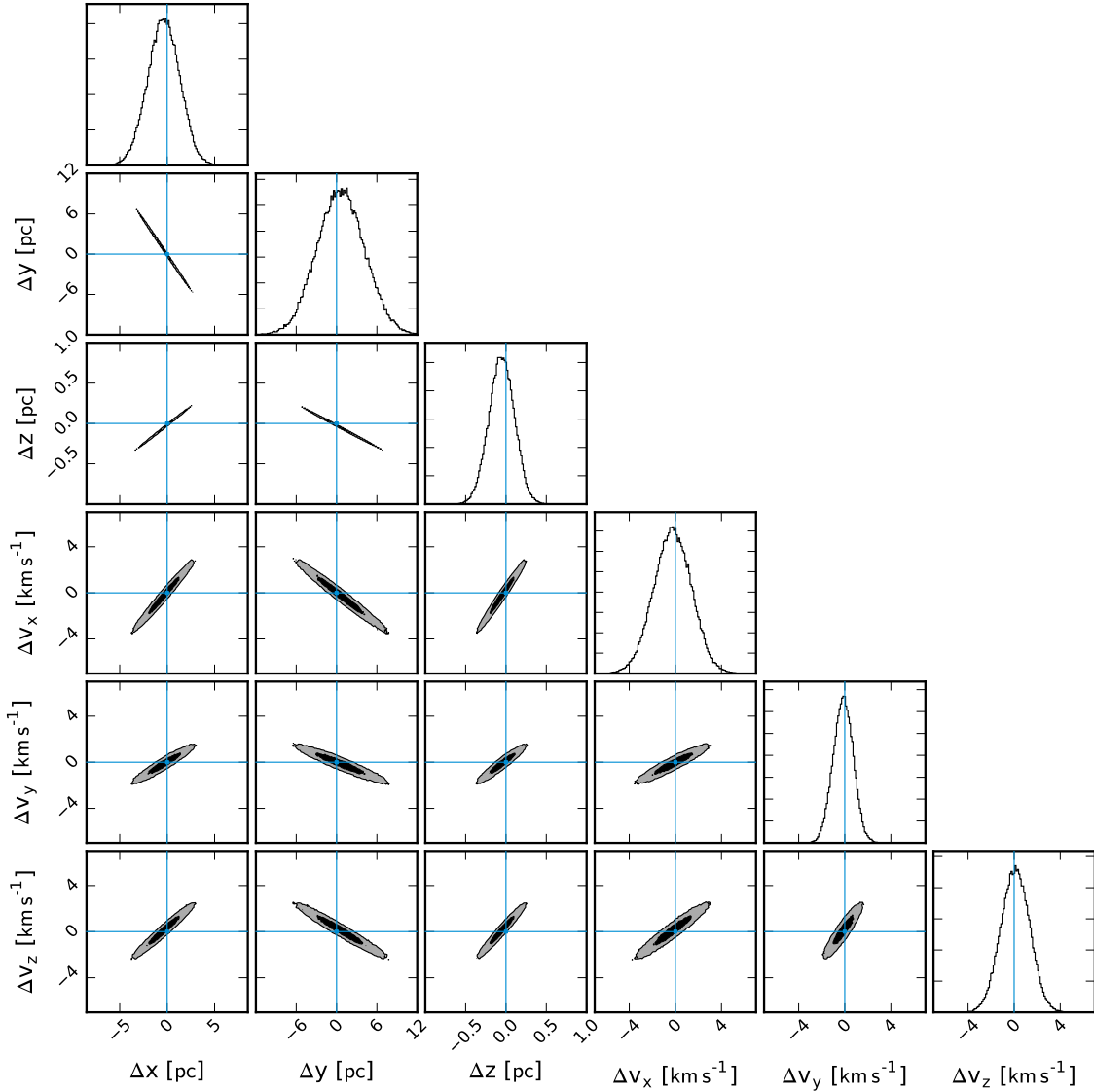


Figure 1. Differences in posterior samples over Galactocentric phase-space coordinates for the two stars Krios and Kronos.

likelihood ratio (Bayes factor) between the two hypotheses is $\ln \mathcal{L}_1/\mathcal{L}_2 = 8.52$, well above the adopted cut value of 6. The pair has also been previously recognized as a visual double star system in Washington Double Star catalog (Mason et al. 2001). We have checked that we do not find any possible additional comoving companions by lowering the likelihood ratio cut for the stars around this pair.

In a separate effort to study detailed chemical abundances of potential planet-hosting stars, high-resolution spectra of both stars were obtained using the HIRES spectrograph on the Keck I telescope, and analyzed (Brewer et al. 2016). The spectral resolution is $R \approx 70000$ and the wavelength coverage is 5164–7799 Å. A typical signal-to-noise ratio in the spectral continuum is > 200 per pixel. The resulting measurements include elemental abundances for 15 chemical species (C, N, O, Na, Mg, Al, Si, Ca,

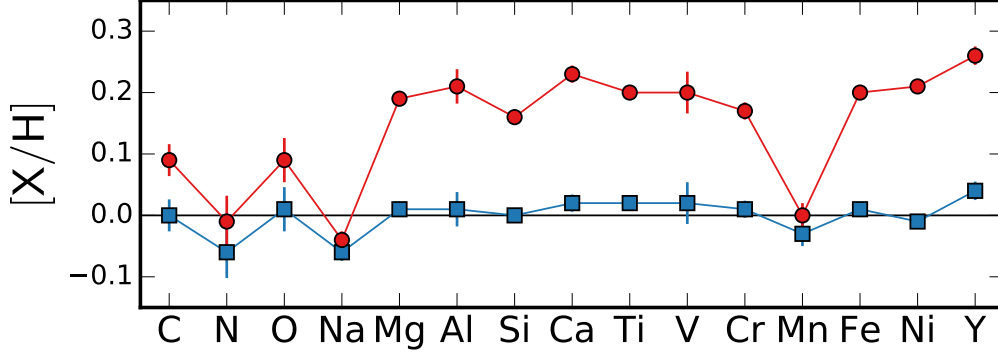


Figure 2. Abundances of the comoving pair, Krios (blue) and Kronos (red). Lines are drawn for each star only to guide the eye. Kronos is enhanced in Fe by ≈ 0.2 dex relative to Krios along with Mg, Al, Si, Ca, Ti, V, Cr, Ni, Y yet not in C, N, O, Na, and Mn.

Ti, V, Cr, Mn, Fe, Ni, Y) as well as stellar parameters and high precision radial velocities. For the details of the spectral analysis, we refer the readers to Brewer et al. 2016. Additionally, the Li doublet at 6707.6 Å for this sample was investigated in a separate work (Myles 2017 in prep). We list all relevant astrometric and spectroscopic measurements including the absolute abundances of Li for the two stars in Table 1.

The projected separation between the pair is $1.9'$ (≈ 0.01 pc), and the 3D separation is ≈ 0.6 pc. Although selected based only on their astrometry, the two stars have identical radial velocities within their uncertainties (Table 1), confirming that they are truly comoving. Combining these precise radial velocities with the *Gaia* TGAS astrometry, we can compare differences between the inferred 6D phase-space coordinates of the two stars. We start by generating posterior samples over the Heliocentric distance, r , tangential velocities, $(v_{\alpha^*}, v_{\delta})$, and radial velocity, v_r , given the observed parallax, $\hat{\pi}$, proper motions, $(\hat{\mu}_{\alpha^*}, \hat{\mu}_{\delta})$, and radial velocity, \hat{v}_r ¹. We assume the noise is Gaussian, and the radial velocity measurements are uncorrelated with the astrometric measurements. If we define

$$\hat{\mathbf{y}} = \left(\hat{\pi} \quad \hat{\mu}_{\alpha^*} \quad \hat{\mu}_{\delta} \quad \hat{v}_r \right)^{\text{T}} \quad (1)$$

$$\mathbf{y} = \left(r^{-1} \quad r^{-1} v_{\alpha} \quad r^{-1} v_{\delta} \quad v_r \right)^{\text{T}} \quad (2)$$

then the likelihood is

$$\hat{\mathbf{y}} \sim \mathcal{N}(\mathbf{y}, \mathbf{C}) \quad (3)$$

where \mathbf{C} is the covariance matrix. We adopt a uniform space density prior for the distance and an isotropic Gaussian for any velocity component, v , with a dispersion

¹ α^* denotes the projection in right ascension direction, i.e., $\mu_{\alpha^*} = \dot{\alpha} \cos \delta$.

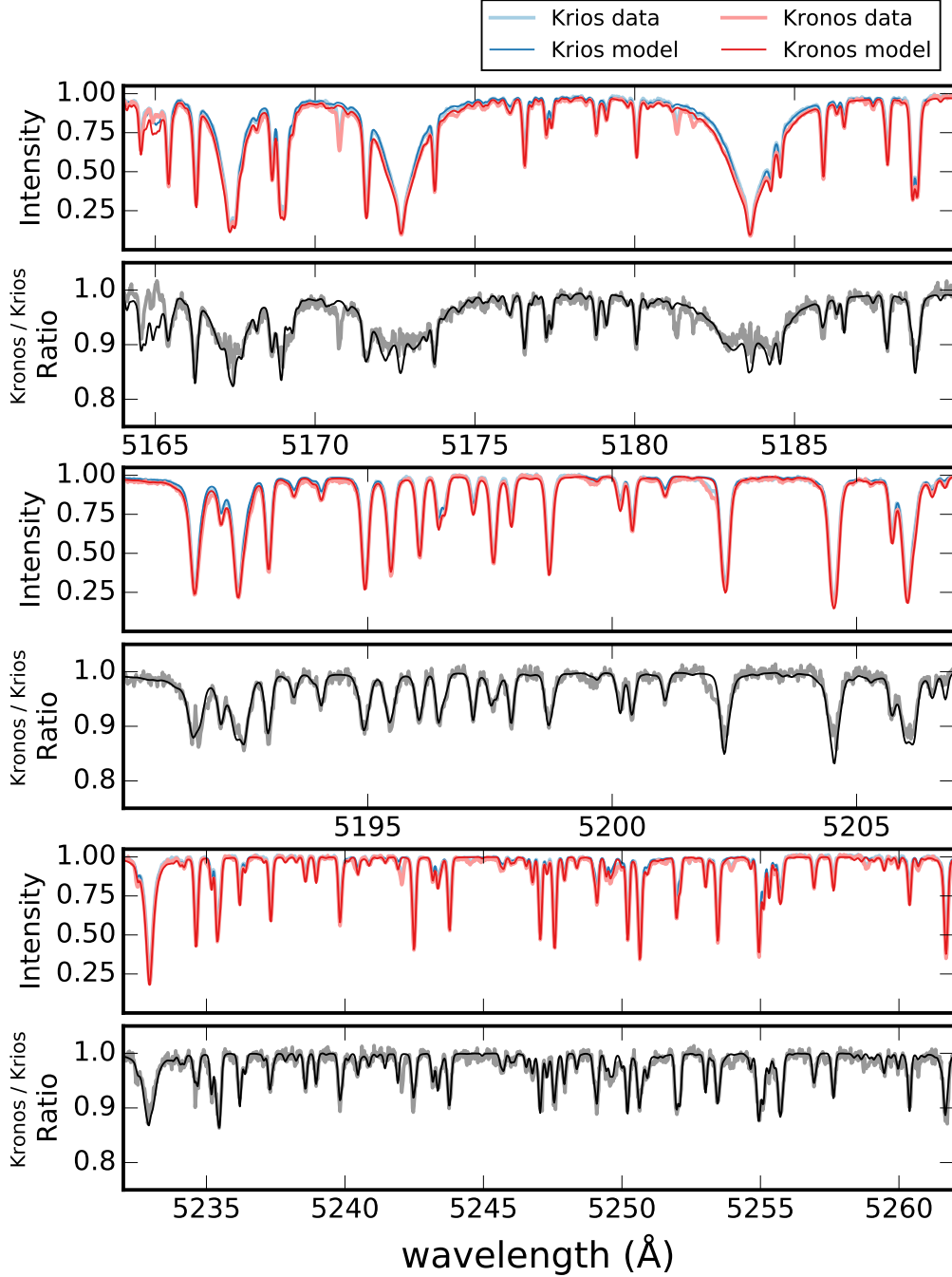


Figure 3. Selective segments of the spectra of Krios and Kronos. Alternating sets of two rows show the continuum-normalized data and model in the upper panel, and the ratio (Kronos/Krios) of data (gray) and model (black) in the lower panel.

$$\sigma_v = 25 \text{ km s}^{-1}$$

$$p(r) = \begin{cases} \frac{3}{r_{\text{lim}}^3} r^2 & \text{if } 0 < r < r_{\text{lim}} \\ 0 & \text{otherwise} \end{cases} \quad (4)$$

$$p(v) = \frac{1}{\sqrt{2\pi} \sigma_v} \exp \left[-\frac{1}{2} \frac{v^2}{\sigma_v^2} \right] \quad (5)$$

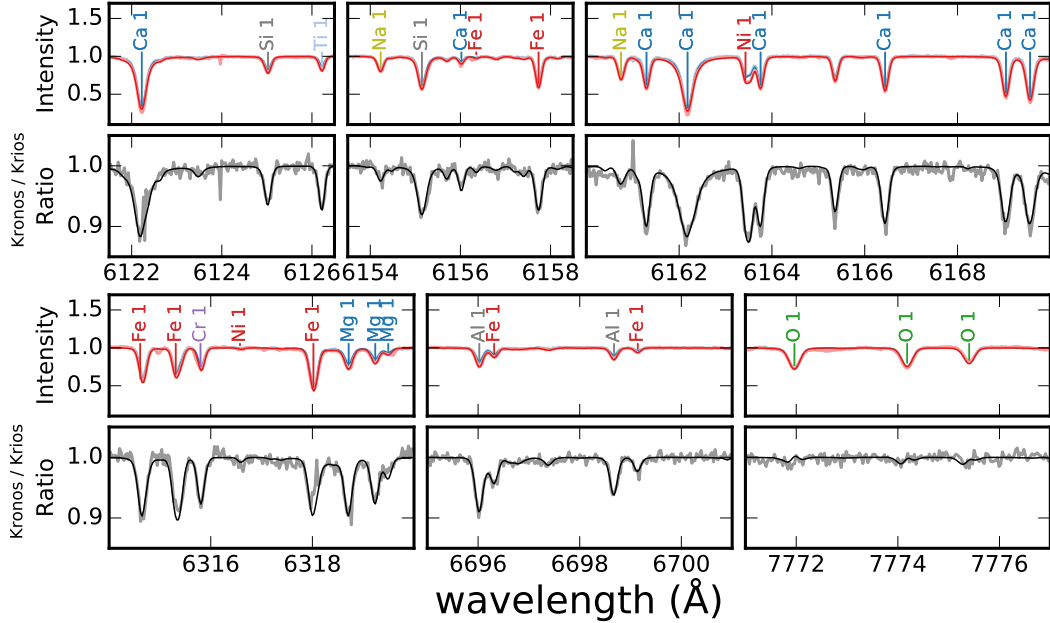


Figure 4. Same as Figure 3 but for smaller portions of spectra at longer wavelengths that are not dominated by Fe. We mark elements that give rise to strong absorption lines. Note that the lines of Na and O, which are under-enhanced in Kronos relative to Fe or other refractory elements, show weaker residuals.

For each of the two stars, we use *emcee* (Foreman-Mackey et al. 2013) to generate posterior samples in $(r, v_\alpha, v_\delta, v_r)$ by running 64 walkers for 4608 steps and discarding the first 512 steps as the burn-in period. For each sample, we convert the heliocentric phase-space coordinates into Galactocentric coordinates assuming that the Sun’s position and velocity are $\mathbf{x}_\odot = (-8.3, 0, 0)$ kpc and $\mathbf{v}_\odot = (-11.1, 244, 7.25)$ km s⁻¹ (e.g., Schönrich et al. 2010; Schönrich 2012).

Figure 1 shows differences in posterior samples converted to Galactocentric phase-space coordinates for the two stars. The differences in velocities are consistent with zero. For a 2 M_⊙ binary system, the Jacobi radius in the Solar neighborhood is 1.2 pc (Jiang & Tremaine 2010). Thus, Kronos and Krios are likely a bound system that formed coevally, and we expect the two stars to have identical metallicities and abundance patterns. However, one of the stars, Kronos is significantly more metal rich than the other by 0.2 dex ($\approx 60\%$; Figure 2). Moreover, not all elements are equally enhanced: the abundances of Kronos show selective depletion in C, N, O, Na, and Mn relative to Fe. Kronos also has a high surface Li abundances, and the difference in Li abundance (≈ 0.5 dex) is the largest among all elements measured.

The validity of the measured abundance differences is further demonstrated in Figure 3, 4, and 5, where we show segments of the spectra and models of the two stars used to measure their abundances (Brewer et al. 2016). As expected from their reported metallicity difference ($\Delta[\text{Fe}/\text{H}] \approx 0.2$), the ratio of data and model between the two stars show significant residuals for almost all metal line features, largely

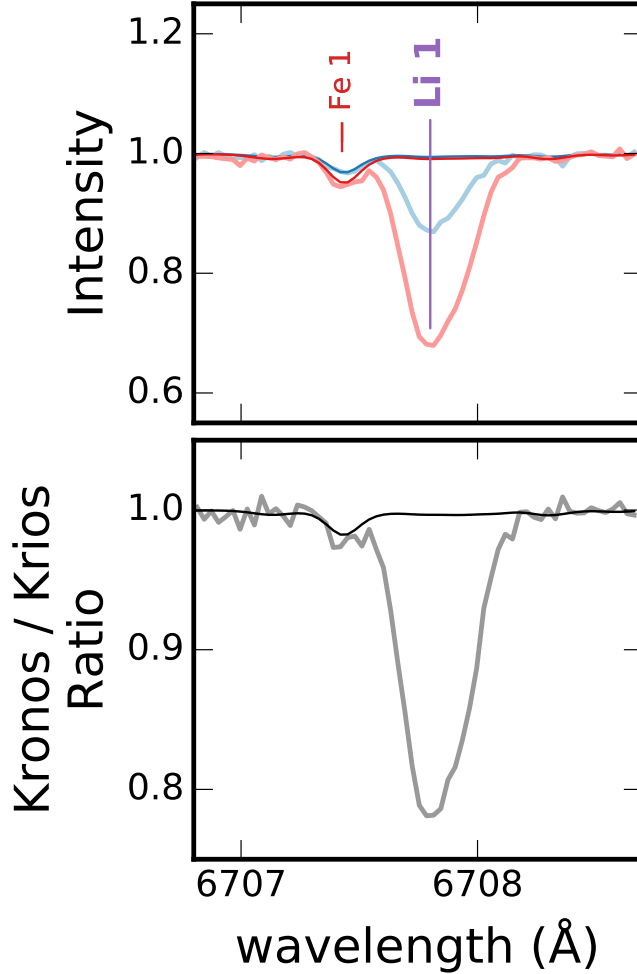


Figure 5. Lithium lines in the spectra of Kronos and Krios. This line is studied in Myles *et al.* (in prep.). Line legends are the same as in Figure 3.

dominated by Fe. However, for lines of elements that are not as enhanced in Kronos the residuals are much smaller in amplitude (Figure 4). The Li doublet, analyzed in a separate work (Myles *et al.* in prep.), is clearly visible in the spectra of both stars, and is stronger in Kronos (Figure 5).

We stress that none of the other four twin-like ($\Delta T_{\text{eff}} \lesssim 100$ K) wide binary pairs examined by Brewer *et al.* 2016 show discrepancies in abundances between the stars at this level. As shown in Figure 6, the differences in other pairs for all elements except N and O, which are also the most uncertain (Table 1), are less than 0.05 dex, making Kronos-Krios pair a significant outlier. The statistical uncertainties for each parameter presented in Table 1 from Brewer *et al.* 2016 are estimated from repeated measurements of multiple spectra of the same stars. We note that while there may be systematic uncertainties (bias) in the elemental abundances of these two stars unconstrained by this procedure, the systematic uncertainties, if any, for these two

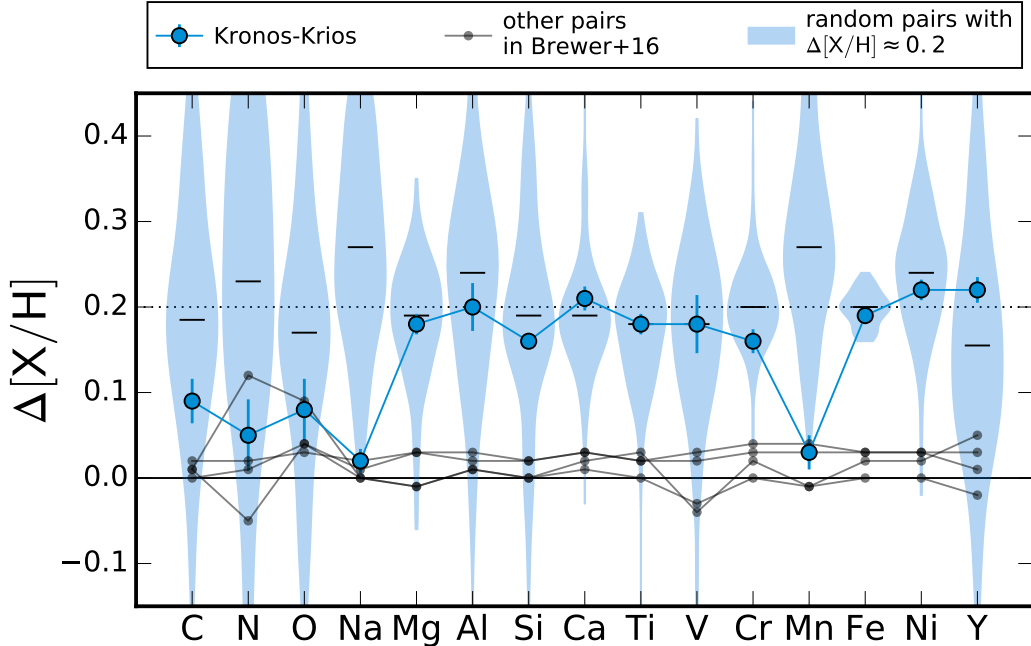


Figure 6. Abundance difference in this pair and other twin-like ($\Delta T_{\text{eff}} \lesssim 100$ K) wide binaries in Brewer et al. 2016. The differences in other pairs are small (< 0.05 dex) for all elements except N and O which are the most uncertain, making the difference of ≈ 0.2 dex seen in Kronos-Krios rare. Additionally, we show the distribution of abundance differences between field stars with similar metallicity difference ($\Delta[\text{Fe}/\text{H}] \approx 0.2$) as violins with medians indicated by black line segments. These are random pairings of single stars in in Brewer et al. 2016 at two metallicity bins, $-0.025 < [\text{Fe}/\text{H}] < 0.025$ (160 stars) and $0.175 > [\text{Fe}/\text{H}] > 0.225$ (137 stars), similar to Kronos and Krios. The difference is always taken to be higher $[\text{Fe}/\text{H}] - \text{lower} [\text{Fe}/\text{H}]$. Thus, the narrower range of $\Delta[\text{Fe}/\text{H}]$ is by construction. Random pairings of disk stars with similar $\Delta[\text{Fe}/\text{H}]$ usually show similar enhancement in all other elements unlike the pattern seen in Kronos-Krios pair.

solar-type “twin-like” stars with small differences in T_{eff} and $\log g$ are unlikely to wash out the observed abundance differences of ≈ 0.2 dex.

3. DISCUSSION

We discuss the possible origins of the peculiar abundance differences of Kronos & Krios. We first discuss the ages and coevality of the stars in this pair, and consider both possibilities in which the two stars are or are not coeval. Our favored scenario is discussed in the last subsection, Section 3.4.

3.1. *Stellar Ages & Coevality*

Apart from their closeness in phase-space coordinates, we can constrain the ages of the two stars given the precise measurements of $\log(g)$ and T_{eff} by comparing these values to theoretical isochrones. We use the distances (inferred from *Gaia* parallaxes), V -band magnitudes, and $B - V$ colors to obtain bolometric luminosities of the two stars (VandenBerg & Clem 2003). We then combine the luminosities with effective temperature, $[\text{Fe}/\text{H}]$, and $[\text{Si}/\text{H}]$ in order to interpolate the age, mass, and radius of

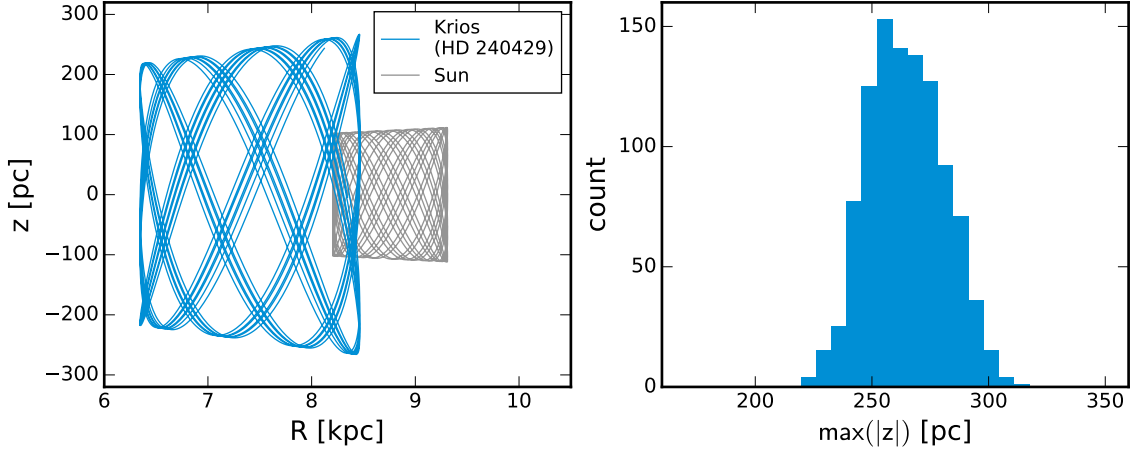


Figure 7. Left panel: Galactic orbits computed for Krios (black) and the Sun (grey). For Krios, the initial conditions are set to the median of the posterior samples over the phase-space coordinates. The orbits are computed by integrating backwards from the present-day positions for 2.5 Gyr with a time step of 0.5 Myr using the Leapfrog integration scheme implemented in *Gala* (Price-Whelan et al. 2017). Right panel: distribution of maximum z -heights for orbits computed from all posterior samples.

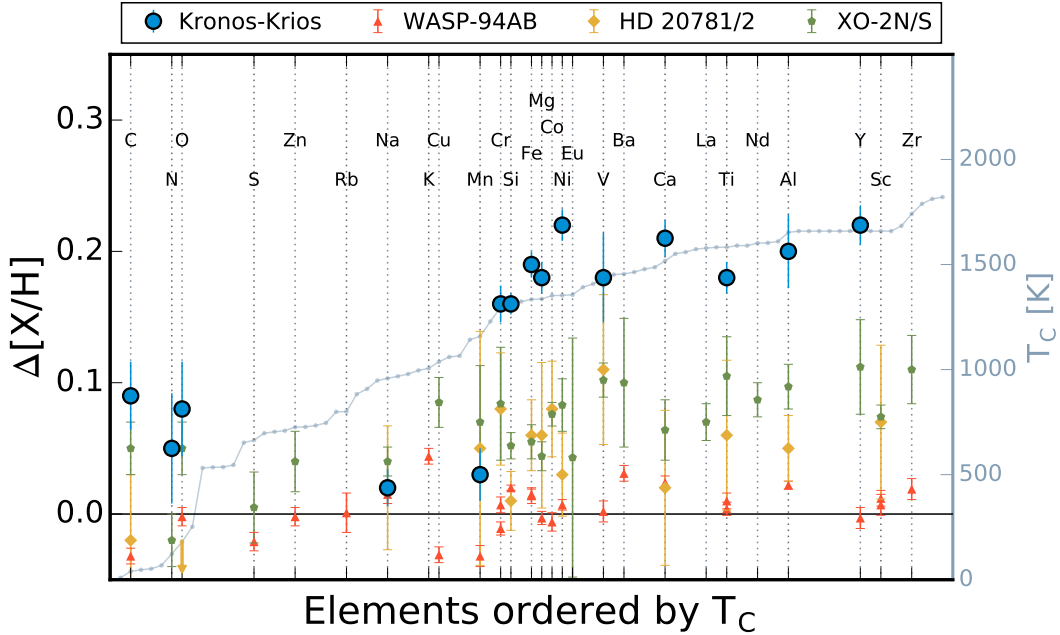


Figure 8. Abundance differences of the Kronos-Krios pair ranked by the condensation temperature of elements for solar composition gas from Lodders 2003. The condensation temperature may be read from the gray line and right y-axis. We show three wide binary systems selected from the literature: HD 20782/1 (Mack et al. 2014, $[\text{Fe}/\text{H}] \approx 0$), XO-2N/S (Biazzo et al. 2015, $[\text{Fe}/\text{H}] \approx 0.35$), and WASP-94AB (Teske et al. 2016a, $[\text{Fe}/\text{H}] \approx 0.3$). Locations of elements with at least one measurement from any study are indicated by a vertical line and its symbol. Note that often multiple values are reported for one element corresponding to different ionization states in equivalent width analyses. No other pair studied so far were shown to have such large difference in metallicity or sharp contrast between (moderately) volatile and refractory elements as Kronos-Krios.

each star using a grid of Yale-Yonsei model isochrones (Spada et al. 2013). The best-fit isochrone ages of Kronos and Krios are $4.28_{-1.03}^{+1.11}$ Gyr and $4.00_{-1.56}^{+1.51}$ Gyr, respectively, consistent with them being coeval.

The surface lithium abundance in a Sun-like star decreases with its age due to mixing induced by convection or rotation, which brings the lithium into the interior ($T > 2.5 \times 10^6$ K) where it will be destroyed by proton capture burning. In hotter stars with thin convective zones on the main sequence, most of this mixing occurs in the pre-main sequence phase when the star is fully convective. Thus, surface lithium abundance can be an indicator of stellar ages, especially whether the star is very young ($\lesssim 1$ Gyr). The absolute Li abundance of solar-type stars also correlates steeply with the effective temperature (e.g., Chen et al. 2001; Ramírez et al. 2012). Generally, cooler stars with larger convective envelope have lower Li abundances. The absolute Li abundance of 2.25 dex for Krios is typical for its T_{eff} . On the other hand, the lithium abundance ($A(\text{Li}) = 2.75$) of Kronos, which has lower T_{eff} than Krios, is not only higher than that of Krios but also much higher compared to other field stars of similar T_{eff} . Given the overall higher metal abundances and the peculiar abundance patterns in Kronos, it is unclear, however, whether this higher Li abundance means a younger age or something else. For example, Casey et al. 2016 attributes the presence of Li-rich red giant stars to the engulfment of substellar companions such as gas giant planets or brown dwarfs which may replenish Li.

The surface lithium abundance of Kronos is the only indicator of a younger age. If the two stars were only several hundred Myrs old, then they may have been part of a larger comoving group of stars. However, as we mention above (Section 2), there is no evidence in our search of comoving pairs using TGAS that the two stars belong to a larger group of young stars. Very young stars often show signs of activity such as X-ray emission from magnetic activity, emission lines, or infrared excess due to circumstellar disks (Feigelson & Montmerle 1999; Adams et al. 1987). We have compiled GALEX, Tycho-2, 2MASS, and WISE photometry for these stars, and found no evidence for indications of activity in their spectral energy distributions. The low $v \sin(i)$ values (Table 1) also argue against very young ages that would be inferred from the surface lithium abundance. Finally, we computed the Galactic orbit of the pair using the median of the posterior sample over the phase-space coordinates of Krios, in a Milky Way-like gravitational potential (similar to `MWPotential2014` from Bovy 2015) using *Gala* (Price-Whelan et al. 2017). The pair’s fiducial orbit has a vertical action larger than the Sun, favoring an older age (Wielen 1977; Aumer et al. 2016). We therefore conclude that the two stars are most likely coeval, ~ 4 Gyr old main sequence stars, and that the unusually high Li abundance of Kronos requires an alternative explanation.

3.2. Exchange Scattering

While the data described above strongly suggests that the two stars are coeval, this subsection explores the possibility that this pair is still not a primordial binary. Two

stars unrelated at birth may end up in a binary system via a binary-single scattering event that results in an exchange of binary members. In order to estimate the rate at which any binary-single event will produce a wide binary system such as Krios and Kronos, we may consider the rate at which this wide binary will scatter with a field star to result in an exchange reaction. The cross-section of exchange scattering for a binary with semi-major axis a is

$$\sigma_{\text{ex}} = \frac{640}{81} \pi a^2 \left(\frac{v_i}{v_c} \right)^{-6} \quad (6)$$

where v_i is the incoming velocity, and v_c is the critical velocity, defined as

$$v_c^2 = G \frac{m_1 m_2 (m_1 + m_2 + m_3)}{m_3 (m_1 + m_2)} \frac{1}{a}. \quad (7)$$

Equation 6 is appropriate when $v_i/v_c \gg 1$ (Hut & Bahcall 1983; Hut 1983), which is the case for wide binaries scattering with field (disk) stars. If we assume that field stars are made of solar-mass stars with a constant number density $n = 1 \text{ pc}^{-3}$, and the incoming velocity of field stars is 10 km s^{-1} , the rate of exchange scattering is

$$n \sigma_{\text{ex}} v_i = 6.82 \times 10^{-8} \text{ Gyr}^{-1} \frac{n}{\text{pc}^{-3}} \frac{\text{pc}}{a} \left(\frac{10 \text{ km s}^{-1}}{v_i} \right)^5, \quad (8)$$

low enough to be negligible.

An exchange scattering scenario is unlikely to be able to explain the observed abundance difference pattern of Kronos and Krios. We test this by randomly drawing pairs of stars in the sample of Brewer et al. 2016 from two $[\text{Fe}/\text{H}]$ bins at $[\text{Fe}/\text{H}] = 0 \pm 0.025$ and $[\text{Fe}/\text{H}] = 0.2 \pm 0.025$, each similar to Krios and Kronos. In Figure 6, we compare the observed abundance difference of Kronos-Krios with the distribution of abundance differences from 300 random pairs. We see that when a star is enhanced in Fe by 0.2 dex, all other elements are typically enhanced at a similar level, with some variations. Specifically, for a typical star with $[\text{Fe}/\text{H}] \approx 0.2$ dex, we generally expect $[\text{Na}/\text{Fe}] > 0$ and $[\text{Mn}/\text{Fe}] > -0.1$ (Battistini & Bensby 2015; Bensby et al. 2003) making the low $[\text{Na}/\text{Fe}]$ and $[\text{Mn}/\text{Fe}]$ seen in Kronos very unlikely to arise from variations in Galactic chemical evolution.

3.3. Chemical Inhomogeneity in Star Formation

In this subsection, we explore the hypothesis that chemical inhomogeneity within the birth cloud is the source of the observed abundance difference. There is ample evidence against this scenario as most wide binaries show a difference in $[\text{Fe}/\text{H}]$ less than 0.02 dex (Desidera et al. 2004; Gratton et al. 2001). Even when a significant difference is detected with high-precision abundance measurements, the difference is typically ~ 0.05 dex (see Figure 8 and Section A). Consistent with these results, none of the other seven similar wide binaries examined in Brewer et al. 2016 show such

large differences in abundances though there is generally a larger spread in C, N and O, and some pairs show a difference in particular elements as large as ≈ 0.15 dex. The median and maximum $[\text{Fe}/\text{H}]$ difference between component stars in the other seven pairs is 0.02 dex and 0.09 dex, respectively. The differences are even smaller (maximum $\Delta[\text{Fe}/\text{H}] = 0.03$ dex) if we compare only twin-like ($\Delta T_{\text{eff}} \lesssim 100$ K) pairs (Figure 6, black lines). Thus, a difference of ≈ 0.2 dex seen in Kronos-Krios pair is unlikely to be due to chemical inhomogeneity in the birth cloud.

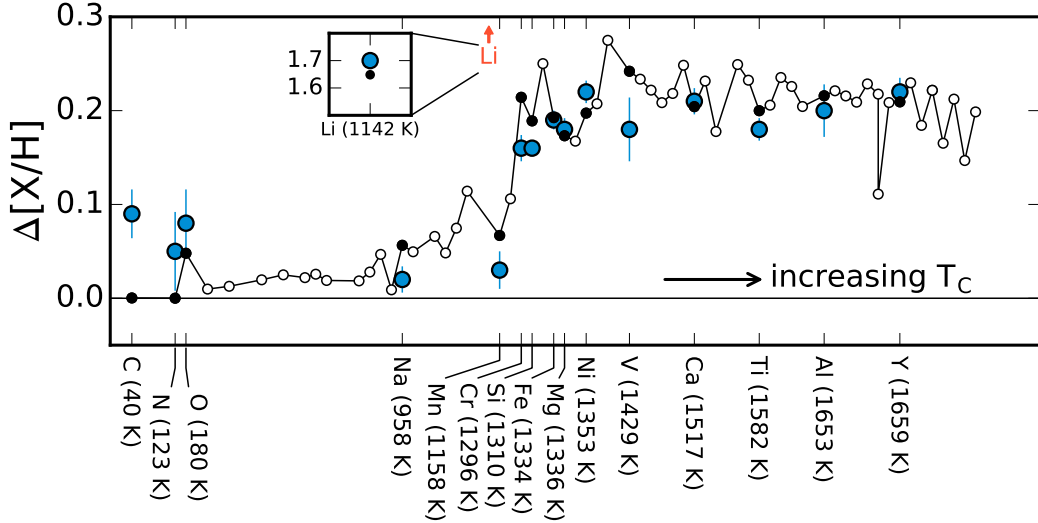


Figure 9. Comparing the observed abundance difference (Kronos – Krios; blue circles) to the expected change in solar surface abundance after adding $15 M_{\oplus}$ of material with bulk Earth composition (McDonough 2003; black open and filled circles). The assumed mass fraction in the convective zone is 0.02. All astronomical metals are ordered by their T_C for solar composition gas on the x -axis. For the predictions, we highlight elements measured for Kronos-Krios pair in filled circles, while those without a measurement are left open. The close match with the observed abundance difference in Kronos-Krios pair suggests that the abundance difference may be due to accretion of $15 M_{\oplus}$ of rocky planetary material. The element Li is off the plot and indicated in the inset.

3.4. Accretion of rocky planetary material

Another possibility that two coeval stars may end up with different surface abundances is accretion of planetary material after birth. In a multi-planet system, dynamical instabilities triggered by planet-planet scattering (Rasio & Ford 1996; Weidenschilling & Marzari 1996) or encounters with a field star (Malmberg et al. 2011) can lead to planet ejection or accretion. Indeed, it is an important goal of many exoplanet studies to detect chemical signatures of planet formation or accretion, distinguish them from Galactic chemical evolution, and connect them to theories of evolution of planetary systems. One approach that is free from confusion with Galactic chemical evolution is to compare two almost identical stars in a wide binary system. Assuming that the component stars were born together with identical initial composition, we may see a difference in their surface abundances if the two stars then accreted different

amounts of planetary material. The resulting abundance difference may depend on the condensation temperatures of elements in the protoplanetary disks from which the accreted planets formed, as their compositions depend on the radial temperature gradient in the disk.

In Figure 8, we show the abundance difference between Kronos and Krios ordered by the rank of T_C of each element. The equilibrium condensation temperatures for the composition of solar system are taken from Lodders 2003 (Table 8). The difference seen in Kronos-Krios is compared to HD 20781/2, XO-2N/S, WASP-94A/B in Figure 8. The metallicity difference of ≈ 0.2 dex observed in this pair is larger than the differences seen in any other pairs studied so far (see also Appendix A). The five under-enhanced elements in Kronos relative to Krios are the five most volatile in all elements measured. The difference in Mn ($T_C = 1158$ K) and Cr ($T_C = 1296$ K) suggests a break in $T_C \approx 1200$ K. This T_C -dependent trend of $\Delta[X/H]$, combined with the enhanced Li abundance ($A(\text{Li}) = 2.75$), strongly suggests that accretion of rocky material has occurred in Kronos.

How much mass of rocky material is needed to explain an increment of ≈ 0.2 dex? We carry out simple toy calculations of the expected $\Delta[X/H]$ in a Sun-like star’s atmosphere by adding a certain mass of bulk Earth composition under these simplifying assumptions:

- The material added is instantly and completely mixed through the star’s convective zone.
- The atmospheric composition that we measure is identical throughout the star’s radiative and convective zone.
- The surface abundance of the star has been altered only by the accretion event(s).

We take the solar abundances, $[X/H]$, of element X (Asplund et al. 2009) which can be converted to mass fraction as

$$f_{X,\text{photo}} = \frac{10^{[X/H]} m_X}{\sum_X 10^{[X/H]} m_X} \quad (9)$$

where m_X is the mass of each element in, e.g., atomic mass unit. Assuming that the accreted material has a total mass M_{acc} , and the mass fraction in each element $f_{X,\text{acc}}$, the abundance difference is

$$\Delta[X/H] = \log_{10} \frac{f_{X,\text{photo}} f_{\text{CZ}} M_{\text{star}} + f_{X,\text{acc}} M_{\text{acc}}}{f_{X,\text{photo}} f_{\text{CZ}} M_{\text{star}}} \quad (10)$$

where f_{CZ} is the fraction of the star’s mass in the convective envelope. We assume $f_{\text{CZ}} = 0.02$ (Spada et al. 2013), and take the composition of bulk Earth from a chondritic model of the Earth (McDonough 2003). Similar calculations have been performed by, e.g., Chambers (2010), Mack et al. (2014, 2016).

Figure 9 shows the expected change of surface abundances of metals in a Sun-like star after $15 M_{\oplus}$ of material with composition of bulk Earth is added. A volatility trend such that more volatile (low T_C) elements are more depleted in the Earth relative to CI or other carbonaceous chondrites has long been known (McDonough 2001). This trend is presumed to be closely related to the formation of terrestrial planets and, in particular, to the radial temperature gradient in a protoplanetary disk. The trend resulting from adding $15 M_{\oplus}$ of bulk Earth provides an overall good match to the observed $\Delta[X/H]$, suggesting that the refractory-enhanced star, Kronos accreted $15 M_{\oplus}$ more of rocky planetary material than Krios.

What about Li? The element Li is worth special attention in the context of the accretion scenario. Because Li is present in either carbonaceous chondrites or bulk Earth with a concentration of 1 – 1.5 ppm in mass (McDonough 2003), but is depleted quickly within the first Gyr on the surface of a Sun-like star (Thévenin et al. 2017; Baraffe et al. 2017), accretion of either material at later times will significantly replenish the lithium on the star’s surface. For the present-day Sun ($A(\text{Li}) = 1.05$), the accretion of $15 M_{\oplus}$ of bulk Earth-like material would result in $\Delta[\text{Li}/\text{H}] \approx 1.65$ dex (see the inset of Figure 9). This closely matches what we find: the Li abundance of Kronos is $A(\text{Li}) = 2.75$ (Table 1, Myles 2017 in prep) approximately 1.7 dex higher than the solar value.

We stress that while the calculation carried out is useful in an order-of-magnitude sense, further investigation of each of the simplifying assumptions made is warranted. In addition, the composition of bulk Earth has some uncertainties. For example, the reported bulk Earth concentration of the siderophile element Mn, varies from 800 to ≈ 2000 ppm (Lodders & Fegley 1998; McDonough 2001, 2003) mainly due to the uncertainty of the Earth’s core composition. Given these limitations, the level of agreement for $\Delta[X/H]$ and Li for Kronos is remarkable.

The fractional mass in the convective zone of solar-type stars decrease dramatically in the first Gyr, and then stays nearly constant at $\approx 2\%$ (Spada et al. 2013). Because the accreted mass M_{acc} is proportional to f_{CZ} , given the large metallicity enhancement (≈ 0.2 dex), the accretion must have happened after a thin convective envelop is established. Otherwise, the accreted mass would be unreasonably high. Thus, it is plausible that a dynamical process after the planet formation ended is responsible for pushing rocky planets in.

Finally, we mention that detection of ${}^6\text{Li}$ provides a strong test for this scenario. This isotope of Li is destroyed at even lower temperatures than ${}^7\text{Li}$, and theoretically expected to be absent (Pinsonneault 1997). However, an accretion of rocky material could have replenished ${}^6\text{Li}$. Because ${}^6\text{Li}$ lines are slightly longer in wavelengths, presence of ${}^6\text{Li}$ increases the asymmetry of Li 6707.6 feature. Depending on how recent the accretion was and how fast ${}^6\text{Li}$ is depleted on the main sequence, this feature may be detectable. This is a very subtle effect that requires a higher signal-to-noise, higher resolution spectra and careful modelling effort (see e.g., Israelian et al. 2001; Reddy

et al. 2002). Such investigation was not warranted by the current data (Myles 2017 in prep).

4. SUMMARY

We report and discuss the discovery of a comoving pair of bright solar-type stars HD 240430 and HD 240429 (G0 and G2) with very different metallicities ($\Delta[\text{Fe}/\text{H}] \approx 0.2$ dex), and condensation temperature (T_C)-dependent abundance differences. The more metal-rich of the two stars, HD 240430 (Kronos), shows enhancement in all ten elements with $T_C > 1200$ K including Fe, while under-enhanced in the five elements, C, N, O, Na, and Mn with $T_C < 1200$ K relative to HD 240429 (Krios). It also has an anomalously high surface Li abundance for its age of ~ 4 Gyr, and its effective temperature very close to that of the Sun. We consider that the comoving pair may have formed from two stars of different birth origins in an exchange scattering event (Section 3.2), or that there may be chemical inhomogeneity in the birth cloud (Section 3.3) to find both unlikely.

In order to explain the T_C -dependent enhancement and high Li abundance of Kronos, we consider the accretion of planetary material as the most plausible cause (Section 3.4). We argue that an accretion of $15 M_{\oplus}$ of bulk Earth composition to Kronos after its thin convective zone is in place can explain the enhancement in both refractory elements and lithium. What triggered the planet engulfment in the two comoving stars remains unclear. One possibility is that a fly-by interaction with a field star could have triggered eccentricity excitation of outer planets, which may have propagated inward through planet-planet scattering, leading to the accretion of inner rocky planets (Zakamska & Tremaine 2004; Malmberg et al. 2011). If this is the case, there may be surviving, highly-eccentric giant planets potentially detectable with future data releases of the *Gaia* mission.

The two stars have not been included in any publicly released data from planet search programs. We have begun a precision radial velocity campaign for the two stars and early indications are that there are no close in giant planets. If both stars have accreted planetary material, it would be very interesting to search for the existence and architectures of the planetary systems left behind.

We thank Andy Casey for bringing ${}^6\text{Li}$ into our attention. We thank Megan Bedell and Andy Casey for valuable discussions, and Keith Hawkins, Nathan Leigh, and Josh Winn for comments on the early version of the draft. The Flatiron Institute is supported by the Simons Foundation.

This work has made use of data from the European Space Agency (ESA) mission *Gaia* (<http://www.cosmos.esa.int/gaia>), processed by the *Gaia* Data Processing and Analysis Consortium (DPAC, <http://www.cosmos.esa.int/web/gaia/dpac/consortium>). Funding for the DPAC has been provided by national institutions, in particular the institutions participating in the *Gaia* Multilateral Agreement. This publication makes use of data products from the Two Micron All Sky Survey, which

is a joint project of the University of Massachusetts and the Infrared Processing and Analysis Center/California Institute of Technology, funded by the National Aeronautics and Space Administration and the National Science Foundation. This publication makes use of data products from the Wide-field Infrared Survey Explorer, which is a joint project of the University of California, Los Angeles, and the Jet Propulsion Laboratory/California Institute of Technology, funded by the National Aeronautics and Space Administration.

Software: This research utilized: `Astropy` (Astropy Collaboration et al. 2013), `corner.py` (Foreman-Mackey 2016), `emcee` (Foreman-Mackey et al. 2013), `IPython` (Pérez & Granger 2007), `matplotlib` (Hunter 2007), `numpy` (Van der Walt et al. 2011), and `pandas` (McKinney 2010).

REFERENCES

- Adams, F. C., Lada, C. J., & Shu, F. H. 1987, *ApJ*, 312, 788
- Allen, C., & Monroy-Rodríguez, M. A. 2014, *ApJ*, 790, 158
- Asplund, M., Grevesse, N., Sauval, A. J., & Scott, P. 2009, *ARA&A*, 47, 481
- Astropy Collaboration, Robitaille, T. P., Tollerud, E. J., et al. 2013, *A&A*, 558, A33
- Aumer, M., Binney, J., & Schönrich, R. 2016, *MNRAS*, 462, 1697
- Baraffe, I., Pratt, J., Goffrey, T., et al. 2017, *ApJL*, 845, L6
- Battistini, C., & Bensby, T. 2015, *A&A*, 577, A9
- Bensby, T., Feltzing, S., & Lundström, I. 2003, *A&A*, 410, 527
- Biazzo, K., Gratton, R., Desidera, S., et al. 2015, *A&A*, 583, A135
- Bovy, J. 2015, *ApJS*, 216, 29
- Brewer, J. M., Fischer, D. A., Basu, S., Valenti, J. A., & Piskunov, N. 2015, *ApJ*, 805, 126
- Brewer, J. M., Fischer, D. A., Valenti, J. A., & Piskunov, N. 2016, *ApJS*, 225, 32
- Casey, A. R., Ruchti, G., Masseron, T., et al. 2016, *MNRAS*, 461, 3336
- Chambers, J. E. 2010, *ApJ*, 724, 92
- Chen, Y. Q., Nissen, P. E., Benoni, T., & Zhao, G. 2001, *A&A*, 371, 943
- Cochran, W. D., Hatzes, A. P., Butler, R. P., & Marcy, G. W. 1997, *ApJ*, 483, 457
- Desidera, S., Gratton, R. G., Scuderi, S., et al. 2004, *A&A*, 420, 683
- Eiroa, C., Fedele, D., Maldonado, J., et al. 2010, *A&A*, 518, L131
- Farihi, J. 2016, *NewAR*, 71, 9
- Farihi, J., Jura, M., & Zuckerman, B. 2009, *ApJ*, 694, 805
- Feigelson, E. D., & Montmerle, T. 1999, *ARA&A*, 37, 363
- Fischer, D. A., & Valenti, J. 2005, *ApJ*, 622, 1102
- Foreman-Mackey, D. 2016, *The Journal of Open Source Software*, 24, doi:10.21105/joss.00024
- Foreman-Mackey, D., Hogg, D. W., Lang, D., & Goodman, J. 2013, *PASP*, 125, 306
- Freeman, K., & Bland-Hawthorn, J. 2002, *ARA&A*, 40, 487
- Graham, J. R., Matthews, K., Neugebauer, G., & Soifer, B. T. 1990, *ApJ*, 357, 216
- Gratton, R. G., Bonanno, G., Claudi, R. U., et al. 2001, *A&A*, 377, 123
- Hunter, J. D. 2007, *Computing In Science & Engineering*, 9, 90
- Hut, P. 1983, *ApJ*, 268, 342
- Hut, P., & Bahcall, J. N. 1983, *ApJ*, 268, 319
- Israelian, G., Santos, N. C., Mayor, M., & Rebolo, R. 2001, *Nature*, 411, 163

- Jensen, E. L. N., Mathieu, R. D., & Fuller, G. A. 1996, *ApJ*, 458, 312
- Jiang, Y.-F., & Tremaine, S. 2010, *MNRAS*, 401, 977
- Kilic, M., von Hippel, T., Leggett, S. K., & Winget, D. E. 2006, *ApJ*, 646, 474
- Klein, B., Jura, M., Koester, D., Zuckerman, B., & Melis, C. 2010, *ApJ*, 709, 950
- Koester, D., Gänsicke, B. T., & Farihi, J. 2014, *A&A*, 566, A34
- Laws, C., & Gonzalez, G. 2001, *ApJ*, 553, 405
- Liu, F., Asplund, M., Ramírez, I., Yong, D., & Meléndez, J. 2014, *MNRAS*, 442, L51
- Lodders, K. 2003, *ApJ*, 591, 1220
- Lodders, K., & Fegley, B. 1998, *The planetary scientist's companion / Katharina Lodders, Bruce Fegley.*
- Mack, III, C. E., Schuler, S. C., Stassun, K. G., & Norris, J. 2014, *ApJ*, 787, 98
- Mack, III, C. E., Stassun, K. G., Schuler, S. C., Hebb, L., & Pepper, J. A. 2016, *ApJ*, 818, 54
- Malmberg, D., Davies, M. B., & Hogg, D. C. 2011, *MNRAS*, 411, 859
- Mason, B. D., Wycoff, G. L., Hartkopf, W. I., Douglass, G. G., & Worley, C. E. 2001, *AJ*, 122, 3466
- Mayer, L., Wadsley, J., Quinn, T., & Stadel, J. 2005, *MNRAS*, 363, 641
- McDonough, W. F. 2001, *International Geophysics*, 76, 3
- McDonough, W. F. 2003, *Treatise on Geochemistry*, 2, 568
- McKinney, W. 2010, in *Proceedings of the 9th Python in Science Conference*, ed. S. van der Walt & J. Millman, 51 – 56
- Meléndez, J., Asplund, M., Gustafsson, B., & Yong, D. 2009, *ApJL*, 704, L66
- Melendez, J., & Ramirez, I. 2016, *ArXiv e-prints*
- Myles, J. e. a. 2017 in prep,
- Oh, S., Price-Whelan, A. M., Hogg, D. W., Morton, T. D., & Spergel, D. N. 2017, *AJ*, 153, 257
- Paquette, C., Pelletier, C., Fontaine, G., & Michaud, G. 1986, *ApJS*, 61, 197
- Patience, J., White, R. J., Ghez, A. M., et al. 2002, *ApJ*, 581, 654
- Pérez, F., & Granger, B. E. 2007, *Computing in Science and Engineering*, 9, 21
- Pinsonneault, M. 1997, *ARA&A*, 35, 557
- Pinsonneault, M. H., DePoy, D. L., & Coffee, M. 2001, *ApJL*, 556, L59
- Price-Whelan, A., Sipocz, B., & Oh, S. 2017, *adrn/gala: v0.1.3*, , , doi:10.5281/zenodo.321907
- Quinn, D. P., Wilkinson, M. I., Irwin, M. J., et al. 2009, *MNRAS*, 396, L11
- Ramírez, I., Fish, J. R., Lambert, D. L., & Allende Prieto, C. 2012, *ApJ*, 756, 46
- Ramírez, I., Meléndez, J., Cornejo, D., Roederer, I. U., & Fish, J. R. 2011, *ApJ*, 740, 76
- Ramírez, I., Khanal, S., Aleo, P., et al. 2015, *ApJ*, 808, 13
- Rasio, F. A., & Ford, E. B. 1996, *Science*, 274, 954
- Reach, W. T., Kuchner, M. J., von Hippel, T., et al. 2005, *ApJL*, 635, L161
- Reddy, B. E., Lambert, D. L., Laws, C., Gonzalez, G., & Covey, K. 2002, *MNRAS*, 335, 1005
- Saffe, C., Flores, M., & Buccino, A. 2015, *A&A*, 582, A17
- Saffe, C., Flores, M., Jaque Arancibia, M., Buccino, A., & Jofré, E. 2016, *A&A*, 588, A81
- Santos, N. C., Israelian, G., & Mayor, M. 2004, *A&A*, 415, 1153
- Schönrich, R. 2012, *MNRAS*, 427, 274
- Schönrich, R., Binney, J., & Dehnen, W. 2010, *MNRAS*, 403, 1829
- Schuler, S. C., Cunha, K., Smith, V. V., et al. 2011, *ApJL*, 737, L32
- Spada, F., Demarque, P., Kim, Y.-C., & Sills, A. 2013, *ApJ*, 776, 87
- Teske, J. K., Ghezzi, L., Cunha, K., et al. 2015, *ApJL*, 801, L10
- Teske, J. K., Khanal, S., & Ramírez, I. 2016a, *ApJ*, 819, 19
- Teske, J. K., Schuler, S. C., Cunha, K., Smith, V. V., & Griffith, C. A. 2013, *ApJL*, 768, L12
- Teske, J. K., Shtetman, S. A., Vogt, S. S., et al. 2016b, *AJ*, 152, 167

- Thévenin, F., Oreshina, A. V., Baturin, V. A., et al. 2017, *A&A*, 598, A64
- Trilling, D. E., Bryden, G., Beichman, C. A., et al. 2008, *ApJ*, 674, 1086
- Tucci Maia, M., Meléndez, J., & Ramírez, I. 2014, *ApJL*, 790, L25
- Udry, S., Dumusque, X., Lovis, C., et al. 2017, *ArXiv e-prints*
- Van der Walt, S., Colbert, S. C., & Varoquaux, G. 2011, *Computing in Science & Engineering*, 13, 22
- VandenBerg, D. A., & Clem, J. L. 2003, *AJ*, 126, 778
- Vanderburg, A., Johnson, J. A., Rappaport, S., et al. 2015, *Nature*, 526, 546
- Weidenschilling, S. J., & Marzari, F. 1996, *Nature*, 384, 619
- Wielen, R. 1977, *A&A*, 60, 263
- Yoo, J., Chanamé, J., & Gould, A. 2004, *ApJ*, 601, 311
- Zakamska, N. L., & Tremaine, S. 2004, *AJ*, 128, 869
- Zuckerman, B., & Becklin, E. E. 1987, *Nature*, 330, 138
- Zuckerman, B., Koester, D., Melis, C., Hansen, B. M., & Jura, M. 2007, *ApJ*, 671, 872
- Zuckerman, B., Koester, D., Reid, I. N., & Hünsch, M. 2003, *ApJ*, 596, 477
- Zuckerman, B., Melis, C., Klein, B., Koester, D., & Jura, M. 2010, *ApJ*, 722, 725

APPENDIX

A. REVIEW OF DETAILED CHEMICAL ABUNDANCE STUDIES OF STARS IN COMOVING PAIRS

We review and summarize a handful of wide binary systems that have been studied in their detailed chemical abundances so far with high-resolution spectroscopy. These systems are 16 Cygni A/B, HD 20782/HD 20781, HD 80606/HD 80607, XO-2N/XO-2S, HAT-P-1, WASP-94A/WASP94-B, and HD 133131A/HD 133131B. We focus on key characteristics of stars and planets, and interpretations of any trend in $\Delta[X/H]$ with T_C . Interested readers may also consult Melendez & Ramirez 2016.

16 Cygni A/B: The chemical composition of this well know pair of solar-type stars (G1.5/G3) has been studied many times. The hotter star 16 Cyg A has no detected planets, but has an M dwarf companion ~ 70 AU away in projected separation which is probably physically associated (Patience et al. 2002), and may have affected planet formation process around the star (Jensen et al. 1996; Mayer et al. 2005). The other star, 16 Cyg B, hosts a giant planet on an eccentric orbit ($e = 0.63$, Cochran et al. 1997). While past measurements of metallicity and abundance difference between the two stars reported conflicting results (Laws & Gonzalez 2001; Schuler et al. 2011), recent studies using high quality spectra (Ramírez et al. 2011; Tucci Maia et al. 2014) consistently reported that A is more metal rich than B by $\approx 0.04 \pm 0.005$ dex. However, there is still a disagreement between studies on whether abundance differences shows a correlation with T_C as well as its interpretation. Tucci Maia et al. 2014 suggested that formation of $1.5 - 6 M_{\oplus}$ rocky core for the giant planet around 16 Cyg B can explain the offset and the positive correlation between $\Delta[X/H](A - B)$ and T_C . On the other hand, Ramírez et al. 2011, who found no correlation, argued that forming giant planets results in an overall shift in all elements.

HD 20782/HD 20781: Two common proper motion G dwarf stars (G2/G9.5) with a projected separation of ~ 9000 AU (corresponding to $4.2'$ sky separation) and solar metallicity host close-in giant planets. HD 20782 hosts a Jupiter-mass planet on a very eccentric ($e \approx 0.97$) orbit with a pericenter distance of 1.4 AU while HD 20781 hosts two Neptune-mass planets within 0.3 AU with moderately high eccentricity ($e \sim 0.1 - 0.3$).² The measured abundances of 15 elements between the two stars are consistent with each other (Mack et al. 2014). However, Mack et al. 2014 argued that there is a moderately significant ($\sim 2\sigma$) positive slope of $\approx 10^{-5}$ dex K^{-1} with increasing T_C for $T_C > 900$ K elements (namely, Na, Mn, Cr, Si, Fe, Mg, Co, Ni, V, Ca, Ti, Al, Sc leaving out C and O of their measurements) in the abundances of each star *individually*. They suggest that this slope is evidence that the stars accreted $10 - 20 M_{\oplus}$ of H-depleted rocky material during giant planet migration.

² The two stars were monitored by *HARPS* campaign, and it has recently been reported by Udry et al. 2017 that HD 20781 hosts four planets between $M \sin(i) \approx 0.006 - 0.04 M_{\text{Jup}}$ with $e \leq 0.11$ within ≈ 0.35 AU.

HAT-P-1: This pair of G0 stars separated by 11'' with $[\text{Fe}/\text{H}] \approx 0.15$ has different planetary systems: the secondary star is known to host one transiting giant planet while no planet has been discovered around the primary star. The two stars are identical in metallicities and abundances for 23 elements measured with the mean error of 0.013 dex (Liu et al. 2014). Thus, it seems that the presence of close-in giant planet does not necessarily lead to atmospheric pollution of its host star.

HD 80606/HD 80607: Similar to HAT-P-1, no significant chemical difference is found between two common proper motion G5 stars with super-solar metallicity ($[\text{Fe}/\text{H}] \approx 0.35$). HD 80606 which hosts a very eccentric ($e \approx 0.94$) giant planet and HD 80607 which has no detected planets (Saffe et al. 2015; Mack et al. 2016).

XO-2N/XO-2S: A few independent studies have investigated this pair of G9 stars with super-solar metallicity ($[\text{Fe}/\text{H}] \gtrsim 0.35$). XO-2N hosts a giant planet while XO-2S is known to host two giant planets with masses $0.26M_{\text{Jup}}$ and $1.37M_{\text{Jup}}$ on moderately eccentric (≈ 0.15) orbits at < 0.5 AU. A significant difference of metallicity ($\gtrsim 0.05$ dex) is detected between the two stars with a possible correlation with T_C (Ramírez et al. 2015; Biazzo et al. 2015 although see also Teske et al. 2015, 2013). At low T_C , the difference (N – S) in volatile elements differ by ~ 0.01 dex while the range of difference spans upto 0.1 dex at $T_C > 1600$ K.

Ramírez et al. 2015 suggested that the small overall depletion (≈ 0.015 dex) of metals in XO-2S compared to XO-2N is plausibly due to the presence of more gas giant planets around XO-2S, following a similar interpretation of Meléndez et al. 2009 of the trend between solar twins and the Sun. In this scenario, forming planets in the protoplanetary disk locks heavier elements to the core of gas giant planets. The positive correlation of $\Delta[\text{X}/\text{H}](\text{N} - \text{S})$ with T_C requires a scenario involving rocky planets. Both forming more rocky planets in XO-2S and accreting more rocky planets to XO-2N at later stage were discussed (Ramírez et al. 2015; Biazzo et al. 2015). The estimated mass of rocky material required to explain the observed trend is a few tens of M_{\oplus} .

WASP-94A/B: Each star in this pair of F8 and F9 stars with super-solar metallicity ($[\text{Fe}/\text{H}] \approx 0.3$) hosts a hot Jupiter. The planet around WASP-94A is transiting with a misaligned, probably retrograde circular ($e < 0.13$) orbit, while that hosted by WASP-94B is a little more massive by $\sim 0.15 M_{\text{Jup}}$ and closer in, aligned with the host star. WASP-94A shows a depletion of 0.02 dex in volatile and moderately volatile elements ($T_C < 1200$ K) and an enhancement of 0.01 dex in refractory elements ($T_C > 1200$ K) relative to WASP-94B, with a median uncertainty of 0.006 dex among all elements resulting in a statistically significant non-zero slope between $\Delta[\text{X}/\text{H}]$ and T_C (Teske et al. 2016a).³ Multiple possibilities related to the formation and evolution of planetary systems around each star as well as causes unrelated to planets such as

³ Note that the condensation temperature T_C used is for solar system composition gas, which can differ from that of higher metallicity gas.

dust cleansing during the fully convective phase or different rotation and granulation between the stars were considered, but none was favored.

ζ^1/ζ^2 Reticuli (HD 20807/HD 20766): With a projected separation of ≈ 3700 AU, both solar-type stars in this pair have no detected planets. However, ζ^2 hosts a debris disk detected via infrared excess (Trilling et al. 2008) as well as direct imaging (Eiroa et al. 2010). Both stars have super-solar metallicity of ≈ 0.2 dex. A differential abundance analysis using high-resolution spectra shows that ζ^1 is more metal rich than ζ^2 by $\sim 0.02 \pm 0.003$ dex, and that there is a positive slope between the abundance differences of 24 species and T_C . A possible explanation proposed is that the relative lack of refractory elements in ζ^2 is because they are locked up in rocky bodies that make up its debris disk (Saffe et al. 2016).

HD 133131A/B: For this metal-poor ($[\text{Fe}/\text{H}] \approx -0.3$), old (~ 9.5 Gyr) pair of solar-type stars, high-precision radial velocity monitoring recently revealed several planets (Teske et al. 2016b): star A hosts two eccentric giant planets at ≈ 1.4 and ≈ 5 AU while star B hosts a longer period giant planet at ≈ 6.5 AU. Teske et al. 2016b measured a deficit of 0.03 ± 0.017 dex in refractory elements in A relative to B without any conclusive interpretation.